

Variable Sampling MPC via Differentiable Time-Warping Function

Zehui Lu, Shaoshuai Mou

Abstract—Designing control inputs for a system that involves dynamical responses in multiple timescales is nontrivial. This paper proposes a parameterized time-warping function to enable a non-uniformly sampling along a prediction horizon given some parameters. The horizon should capture the responses under faster dynamics in the near future and preview the impact from slower dynamics in the distant future. Then a variable sampling MPC (VS-MPC) strategy is proposed to jointly determine optimal control and sampling parameters at each timestamp. VS-MPC adapts how it samples along the horizon and determines optimal control accordingly at each timestamp without offline tuning or trial and error. A numerical example of a wind farm battery energy storage system is also provided to demonstrate that VS-MPC outperforms the uniform sampling MPC.

I. INTRODUCTION

In many applications such as energy management systems, transportation, aerospace systems, and process control systems, a primary task is to make real-time decisions or scheduling while optimizing a specific objective and not violating some constraints [1]. If a dynamical model of such a system is available prior, one commonly used method is model predictive control (MPC) [1]. To formulate an MPC problem, a discrete-time dynamical model of the system is typically required to construct a discrete-time prediction of system behaviors over a specific prediction horizon. To achieve an optimum of a given objective, MPC methods usually explore all possible control inputs while guaranteeing that these control inputs can forward propagate the given dynamics correctly and not violate any given constraints.

When MPC is applied to multi-timescale systems, such as power grids [2], chemical processes [3], aerospace systems [4], [5], and electrified vehicles [6]–[8], the slower dynamics often require a longer prediction horizon. This usually leads to a higher-dimension MPC problem with a larger computational burden. To address this challenge, the singular perturbation theory [9] has been explored broadly, which decomposes a multi-timescale system into two subsystems with faster and slower timescales, respectively. Then an MPC controller can be developed for each of these two subsystems. But this method is only applicable to the systems whose dynamics can be explicitly decomposed into two subsystems with faster and slower timescales.

Another method of controlling multi-timescale systems is hierarchical MPC (H-MPC) [2], [4], [5], [7], [10], [11]. The H-MPC method first computes an optimal reference

by an MPC given slower dynamics over a relatively long prediction horizon. Then, a reference tracking problem is solved by another controller given faster dynamics over a shorted prediction horizon and hence some optimal control inputs can be obtained. Besides time delays arising from communication among controllers, choosing a proper quantity as the reference value requires prior knowledge of the specific system.

Briefly, to make MPC able to deal with multi-timescale systems well, the prediction horizon should be longer to capture more look-ahead information in the distant future yet the sampling rate of MPC should be small enough to provide more accurate prediction in the near future. A multi-horizon MPC (MH-MPC) [8], [12] has been studied recently, which combines a short receding horizon and a long shrinking horizon altogether in one MPC formulation. The short receding horizon indicates relatively accurate prediction with a higher sampling rate, whereas the long shrinking horizon extends to the end of the trip with a lower sampling rate. Even though MH-MPC exploits preview information over a longer horizon, it introduces an extra computational burden, especially at the beginning of the trip, because the dimension of the MH-MPC problem varies and depends on the current progress over the entire trip. In addition, MH-MPC requires the entire trip to be finite. Another direction to develop MPC for multi-timescale systems is by the non-uniform sampling MPC (NS-MPC) [13]–[16], in which the prediction horizon is partitioned into multiple parts and each part has a different sampling rate. The dimension of the decision variables, i.e., the number of prediction steps, is assumed to be fixed to avoid an extra computational footprint. Both NS-MPC and MH-MPC require manual tuning of some parameters to obtain better performance by trial and error. And determining the optimal settings involves trial and error, and requires expert knowledge of the specific system.

Instead of manually tuning some parameters of a prediction horizon, this paper seeks a differentiable temporal mapping from sampling time to actual time such that it can describe any non-uniform sampling under some parameterizations. Time-warping functions represent this kind of mapping, which was originally proposed to deal with the time misalignment between two temporal sequences [17], or between human demonstrations and system observations [18], [19]. To describe the faster dynamics in the near future precisely and preview the impact of the slower dynamics in the distant future, there are some constraints on a time-warping function, which require the function's differentiability. Then the function's parameters can be a part of decision variables to be optimized while designing control inputs at

The authors are with the School of Aeronautics and Astronautics, Purdue University, IN 47907, USA {lu846,mou}@purdue.edu

This work was supported by a gift funding from Northrop Grumman Corporation.

run-time.

To control a multi-timescale system with one MPC controller and avoid the manual tuning of sampling, this paper proposes a variable sampling MPC (VS-MPC) strategy to accurately capture the responses under the faster dynamics in the near future and preview the impact from the slower dynamics in the distant future. In detail, a differentiable time-warping function describes the timeline of a prediction horizon. The function is parameterized by some decision variables and an optimal control problem jointly determines the control inputs and function parameters at each timestamp without any manual tuning on the horizon. As the situation changes at run-time, VS-MPC adapts how it samples along the horizon and then determines optimal control accordingly. In addition, Section IV studies how the proposed VS-MPC strategy performs in a specific application where a control strategy needs to be designed to control a battery energy storage system (BESS) for a wind farm. A performance comparison for several methods is also included in Section IV.

Notation The real number set is \mathbb{R} . The non-negative real number set is $\mathbb{R}_{\geq 0}$. Let $\text{col}\{\mathbf{v}_1, \dots, \mathbf{v}_a\}$ denote a column stack of elements $\mathbf{v}_1, \dots, \mathbf{v}_a$, which may be scalars, vectors or matrices, i.e. $\text{col}\{\mathbf{v}_1, \dots, \mathbf{v}_a\} \triangleq [\mathbf{v}_1' \ \dots \ \mathbf{v}_a']'$. For a scalar $x \in \mathbb{R}$, $[x]^+ \triangleq x$ when $x \geq 0$ and 0 otherwise. $\mathcal{N}(\mu, \sigma^2)$ indicates a normal distribution with a mean μ and a standard deviation σ .

II. PROBLEM FORMULATION

Suppose the continuous-time open-loop system dynamics for a plant are described by

$$\dot{\mathbf{x}}(t) = \mathbf{f}_c(\mathbf{x}(t), \mathbf{u}(t)), \quad (1)$$

where $t \in \mathbb{R}_{\geq 0}$ denotes time, $\mathbf{x}(t) \in \mathbb{R}^n$ denotes state at time t , $\mathbf{u}(t) \in \mathbb{R}^m$ denotes input at time t , and $\mathbf{f}_c : \mathbb{R}^n \times \mathbb{R}^m \times \mathbb{R}^r \mapsto \mathbb{R}^n$ denotes the nonlinear dynamics.

The open-loop control $\mathbf{u}(t)$ is determined by discrete-time model predictive control with sampling in the following way. Let N denote the number of steps in a prediction horizon and \mathbf{x}_k denote the value of $\mathbf{x}(t)$ at the sampling time t_k , $k = 0, 1, 2, \dots$, i.e. $\mathbf{x}_k = \mathbf{x}(t_k)$. By Euler integration with non-uniform sampling time $\Delta_k > 0$ at time t_k , one reaches the following discretization of the continuous system in (1):

$$\mathbf{x}_{k+1} = \mathbf{x}_k + \Delta_k \mathbf{f}_c(\mathbf{x}_k, \mathbf{u}_k). \quad (2)$$

Let

$$J \triangleq J(\mathbf{x}_{0:N|k}, \mathbf{u}_{0:N-1|k}, \Delta_{0:N-1|k}),$$

where $\mathbf{x}_{0:N|k} \triangleq \text{col}\{\mathbf{x}_k, \mathbf{x}_{k+1|k}, \dots, \mathbf{x}_{k+N|k}\} \in \mathbb{R}^{n(N+1)}$ denotes the state at current time t_k and the states from the future time t_{k+1} to t_{k+N} that are predicted at time t_k ; similarly $\mathbf{u}_{0:N-1|k} \triangleq \text{col}\{\mathbf{u}_{k|k}, \dots, \mathbf{u}_{k+N-1|k}\} \in \mathbb{R}^{mN}$; $\Delta_{0:N-1|k} \triangleq \text{col}\{\Delta_{k|k}, \dots, \Delta_{k+N-1|k}\} \in \mathbb{R}^N$ denotes the non-uniform sampling time intervals from time t_k to t_{k+N-1} that are determined at current time t_k . Note that for a uniform sampling, Δ_k is a constant for any time t_k .

Then at time t_k , given the current state \mathbf{x}_k , the optimal control can be determined by

$$\begin{aligned} \min_{\substack{\mathbf{u}_{0:N-1|k} \\ \Delta_{0:N-1|k}}} & J(\mathbf{x}_{0:N|k}, \mathbf{u}_{0:N-1|k}, \Delta_{0:N-1|k}) \\ \text{s.t.} & \quad \mathbf{x}_{k+j+1|k} = \mathbf{x}_{k+j|k} + \Delta_{k+j|k} \mathbf{f}_c(\mathbf{x}_{k+j|k}, \mathbf{u}_{k+j|k}), \\ & \quad \forall j = 0, \dots, N-1 \text{ with given } \mathbf{x}_k, \\ & \quad \mathbf{g}(\mathbf{x}_{0:N|k}, \mathbf{u}_{0:N-1|k}, \Delta_{0:N-1|k}) \leq \mathbf{0}, \\ & \quad \mathbf{h}(\mathbf{x}_{0:N|k}, \mathbf{u}_{0:N-1|k}, \Delta_{0:N-1|k}) = \mathbf{0}, \end{aligned} \quad (3)$$

where $\mathbf{g}(\mathbf{x}_{0:N}, \mathbf{u}_{0:N-1}, \Delta_{0:N-1|k})$ denotes a column stack of inequality constraints; $\mathbf{h}(\mathbf{x}_{0:N}, \mathbf{u}_{0:N-1}, \Delta_{0:N-1|k})$ denotes a column stack of equality constraints; \leq and $=$ in these constraints indicate element-wise inequality and equality. The discrete-time optimal control determined at time k will be denoted by $\mathbf{u}_{0:N-1|k}^*$. Then in a receding horizon fashion, the system will perform the optimal control $\mathbf{u}_{k|k}^*$ at time t_k , update its states at time t_{k+1} , and then rerun the optimal control problem (3) with current state \mathbf{x}_{k+1} . This procedure will be performed repeatedly under a prescribed frequency. Solving (3) repeatedly in a receding-horizon fashion at run-time is unrealistic because determining the sampling rates $\Delta_{0:N-1|k}$ requires offline manual tuning by trial and error for every specific application. The **problem of interest** is to find the discrete-time optimal control $\mathbf{u}_{0:N-1|k}^*$ and sampling steps $\Delta_{0:N-1|k}$ jointly at each time t_k , without any manual tuning of $\Delta_{0:N-1|k}$ afterward.

III. APPROACH

This section introduces a variable sampling MPC (VS-MPC) strategy, which partitions a prediction horizon with non-uniform sampling by a time-warping function. The time-warping function is parameterized by some decision variables and describes the mapping from sampling time to actual time. Then at each timestamp, VS-MPC solves an optimal control problem in which its decision variables consist of the control inputs in (3) and the parameters of the time-warping function. With the situation changing at each timestamp, VS-MPC finds optimal control inputs and sampling settings jointly without manual tuning afterward.

A. Time-warping Function

This paper proposes a differentiable time-warping function $w : \mathbb{R} \mapsto \mathbb{R}$ and denote $t = w(\tau)$, where $\tau \geq 0$ denotes the sampling time and $t \geq 0$ denotes the actual time. The states are sampled at $\tau = 0, 1, \dots$ and the actual time associated with τ are $t = w(0), w(1), \dots$. Some general constraints are considered on this time-warping function:

$$w(0) = 0, \quad \left. \frac{\partial w(\tau)}{\partial \tau} \right|_{\tau=\hat{\tau}} > 0, \quad \forall \hat{\tau} \geq 0 \quad (4)$$

Given the time-warping function $w(\cdot)$ and the formulation of (3), the time interval between two adjacent timestamp is

$$\Delta_j = w(j+1) - w(j).$$

Fig. 1 shows the two most common time warping functions for MPC. The left one indicates a uniform sampling when

formulating an MPC problem, and the right one indicates a non-uniform sampling which partitions the entire horizon into multiple parts. Note that the right one is not differentiable at certain points.

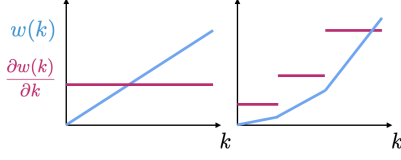


Fig. 1: Two most common time warping functions for MPC

To consider the system's future behavior when developing control, a single optimal control problem is often required to cover a total time T given N steps in the prediction horizon, i.e. $w(N) = T$. To make the prediction horizon adjustable, one can rewrite $w(N) = T$ as

$$\underline{\alpha}T \leq w(N) \leq \bar{\alpha}T, \quad (5)$$

where $\underline{\alpha} > 0$ and $\bar{\alpha} > \underline{\alpha}$. Intuitively, one usually introduces small Δ_k in the near future and larger Δ_k in the distant future, which leads to one additional constraint:

$$\left. \frac{\partial w(\tau)}{\partial \tau} \right|_{\tau=\tau_2} - \left. \frac{\partial w(\tau)}{\partial \tau} \right|_{\tau=\tau_1} \geq 0, \quad \forall \tau_2 \geq \tau_1 \geq 0. \quad (6)$$

Without loss of generality, this paper chooses a polynomial with degree $s = 2$ to represent a time-warping function:

$$t = \hat{w}(\tau, \boldsymbol{\beta}) = \beta_1 \tau + \beta_2 \tau^2,$$

where $\boldsymbol{\beta} = [\beta_1 \ \beta_2]^\top \in \mathbb{R}^s$ is the coefficient vector that parameterizes the time warping function \hat{w} . The constraints (4) and (6) can be rewritten as

$$\begin{aligned} \beta_1 + 2\beta_2 \tau &> 0, \quad \forall \tau \geq 0 \\ 2\beta_2 &\geq 0, \quad \forall \tau \geq 0. \end{aligned} \quad (7)$$

Thus the parameter $\boldsymbol{\beta}$ should satisfy the following conditions:

$$\begin{aligned} \underline{\alpha}T &\leq \hat{w}(N, \boldsymbol{\beta}) \leq \bar{\alpha}T, \\ \beta_1 &> 0, \quad \beta_2 \geq 0. \end{aligned} \quad (8)$$

Note that at time t_k , the current time warping function $\hat{w}_k(\tau, \boldsymbol{\beta}) = \hat{w}(\tau, \boldsymbol{\beta}) + t_k$ and $\frac{\partial \hat{w}_k(\tau, \boldsymbol{\beta})}{\partial \tau} = \frac{\partial \hat{w}(\tau, \boldsymbol{\beta})}{\partial \tau}$.

A parameterized time-warping function with a larger s can represent a more complicated time mapping. However, it is impossible to construct constraints on $\boldsymbol{\beta}$ such that the conditions (4) and (6) are satisfied when $s \geq 6$ because there is no algebraic solution to general polynomial equations of degree five or higher with arbitrary coefficients, as per Abel–Ruffini Theorem [20]. Hence, one cannot obtain a constraint for $\boldsymbol{\beta} \in \mathbb{R}^s$ to satisfy (7) when $s \geq 6$.

Although a polynomial function is used to parameterize the time-warping function, a time-warping function can be any function, as long as the constraints (4), (5), and (6) is satisfied. This paper uses polynomial parameterization due to its simplicity.

B. Variable Sampling MPC

If a non-uniform sampling is determined and well-tuned given the current situation, this sampling is not necessarily suitable for the next timestamp, which can be caused by external disturbance, etc. Variable sampling MPC (VS-MPC) adapts how it samples along the horizon and determines optimal control accordingly at each timestamp t_k , without any offline manual tuning.

The VS-MPC strategy with variable sampling includes an optimal control problem at an arbitrary time t_k , which is formulated as follows:

$$\begin{aligned} \min_{\substack{\mathbf{u}_{0:N-1|k} \\ \boldsymbol{\beta}_k \in \mathbb{R}^2}} & J(\mathbf{x}_{0:N|k}, \mathbf{u}_{0:N-1|k}, \Delta_{0:N-1|k}) \\ \text{s.t.} & \quad \mathbf{x}_{k+j+1|k} = \mathbf{x}_{k+j|k} + \Delta_{k+j|k} \mathbf{f}_c(\mathbf{x}_{k+j|k}, \mathbf{u}_{k+j|k}), \\ & \quad \forall j = 0, \dots, N-1 \text{ with given } \mathbf{x}_k, \\ & \quad \mathbf{g}(\mathbf{x}_{0:N|k}, \mathbf{u}_{0:N-1|k}, \Delta_{0:N-1|k}) \leq \mathbf{0}, \\ & \quad \mathbf{h}(\mathbf{x}_{0:N|k}, \mathbf{u}_{0:N-1|k}, \Delta_{0:N-1|k}) = \mathbf{0}, \\ & \quad \Delta_{k+j|k} = \hat{w}(j+1, \boldsymbol{\beta}_k) - \hat{w}(j, \boldsymbol{\beta}_k), \\ & \quad \forall j = 0, \dots, N-1, \\ & \quad \underline{\alpha}T \leq \hat{w}(N, \boldsymbol{\beta}_k) \leq \bar{\alpha}T, \\ & \quad -\beta_1 < 0, \quad -\beta_2 \leq 0. \end{aligned} \quad (9)$$

At each timestamp t_k , VS-MPC determines the optimal control and how it samples given (9). Then it performs the optimal control and repeats this process in the next timestamp. The detailed explanation of the algorithm for VS-MPC is shown below, where $\frac{1}{dt_{mpc}}$ indicates the MPC frequency. The MPC frequency is typically determined by the specifications of the actual controller.

Algorithm 1: Variable Sampling MPC

Input: $k = 0, t_0, x(t_0), N, dt_{mpc} > 0$

- 1 **while true do**
- 2 $\mathbf{u}_{0:N-1|k}^*, \boldsymbol{\beta}_k^* \leftarrow \text{solve (9)}$
- 3 $\hat{w}_k(\cdot, \boldsymbol{\beta}) = \hat{w}(\cdot, \boldsymbol{\beta}) + t_k$
- 4 $\mathbf{u}_k \leftarrow \text{interpolate } \mathbf{u}_{0:N-1|k}^* \text{ for time } [t_k, t_k + dt_{mpc}] \text{ given } \hat{w}_k(\cdot, \boldsymbol{\beta}) \text{ and zero-order hold}$
- 5 **perform** \mathbf{u}_k **until** $t_k + dt_{mpc}$
- 6 $t_k \leftarrow t_k + dt_{mpc}$
- 7 $k \leftarrow k + 1$

IV. SIMULATIONS

This section shows how the VS-MPC strategy is applied to a battery energy storage system (BESS) for a wind farm and compares the revenue regarding two MPC strategies with uniform sampling and variable sampling.

A. Battery Energy Storage System for Wind Farm

This subsection discusses how to design controls of a BESS by MPC to provide reserves to mitigate wind power intermittency. The following problem formulation originates

from Ref. [21]. In particular, an MPC strategy will be used to control the charge and discharge of the battery in BESS to reduce the negative impact caused by wind intermittency. As shown in Fig. 2, the MPC strategy is required to decide, at each timestamp, how much wind power goes to the power grid and how much goes to the BESS or how much power the BESS discharge and then goes to the grid.

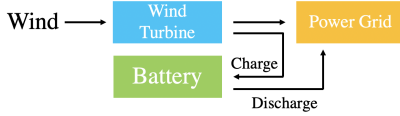


Fig. 2: A battery energy storage system for a wind farm

Assume that the nameplate capacity [MWh] of the wind farm is denoted by $Q_n > 0$. Assuming that the efficiencies of both charge and discharge are perfect, and the responses of both are instantaneously fast, the dynamics of the battery state of charge (SOC) are governed as follows:

$$\dot{x}(t) = -\frac{P_{batt}(t)}{Q_c}, \quad (10)$$

where $x(t) \in [0, 1]$ is the battery SOC at time t ; $P_{batt}(t) \in \mathbb{R}$ is the battery discharge power [MW] and $P_{batt}(t) < 0$ indicates the battery is charging at time t ; $Q_c > 0$ is the battery capacity [MWh].

Suppose that the control input is the scheduling wind power $u(t) \in \mathbb{R}_{\geq 0}$ at time t that goes to the grid and denotes the actual wind power at time t as $w_a(t) \in \mathbb{R}_{\geq 0}$, then $P_{batt}(t) = u(t) - w_a(t)$. The system dynamics of the BESS are written as follows:

$$\dot{x}(t) = f_c(x(t), u(t)) = \frac{w_a(t) - u(t)}{Q_c}. \quad (11)$$

Assume that $w_a(t)$ is unknown before determining the power scheduling $u(t)$ at time t but there is a wind power forecasting $w_f(t) \in \mathbb{R}_{\geq 0}$ available at time t . Then, one needs to determine the power scheduling based on wind power forecasting.

The cost function includes the revenue of selling wind power to the grid, the expense of scheduling conventional reserves based on wind forecasting, the expense of dispatching conventional reserves due to the mismatch between actual and forecasted wind power, and the expense of ramping services [21]. Denote the power reserve requirement at time t_k as $r(u, w_f) = [u(t_k) - w_f(t_k)]^+$ and the wind power shortage due to the imperfect forecasting at time t_k as $d(u, w_a) = [u(t_k) - w_a(t_k)]^+$. Denote $\bar{P}(x_k) \in \mathbb{R}_{\geq 0}$ as the battery discharging power limit given the SOC x_k at time t_k . Similarly, $\underline{P}(x_k) \in \mathbb{R}_{\leq 0}$ denotes the battery charging power limit. Then the cost c_k at time t_k is defined by

$$\begin{aligned} c_k = & -\alpha_1 u_k + \alpha_2 \left[r(u_k, w_f(t_k)) - \bar{P}(x_k) \right]^+ \\ & + \alpha_3 \left[d(u_k, w_a(t_k)) - \bar{P}(x_k) \right]^+ \\ & + \alpha_4 |u_k - u_{k-1}|. \end{aligned} \quad (12)$$

Note that c_k cannot be evaluated at current time t_k because $w_a(t_k)$ is unknown. Instead, the estimated cost $\hat{c}_{k+j|k}$ of time t_{k+j} that is predicted at time t_k is defined as

$$\begin{aligned} \hat{c}_{k+j|k} = & -\alpha_1 u_{k+j|k} + (\alpha_2 + \alpha_3) \left[r(u_{k+j|k}, w_f(t_{j+k})) \right. \\ & \left. - \bar{P}(x_{k+j|k}) \right]^+ + \alpha_4 \ell(u_{k+j|k} - u_{k+j-1|k}), \end{aligned} \quad (13)$$

where $\ell : \mathbb{R} \mapsto \mathbb{R}_{>0}$ denotes a smooth approximation of absolute value function $|\cdot|$ and $\ell(x) = \sqrt{x^2 + 0.01}$. The coefficients $\alpha_1, \alpha_2, \alpha_3$, and α_4 are the unit price of electricity generation, reserve scheduling, reserve dispatch, and ramping services in the wholesale market, respectively. And these coefficients are determined based on statistics in [22], i.e.

$$\alpha_1 = 1, \alpha_2 = 1.03, \alpha_3 = 1, \alpha_4 = 0.5455. \quad (14)$$

Thus, the total estimated cost over time horizon $[t_k, t_{k+N}]$ is defined by

$$\hat{J}_k = \sum_{j=0}^{N-1} \hat{c}_{k+j|k} \Delta_{k+j|k}, \quad (15)$$

where $u_{k-1|k}$ indicates the previous control input at time t_{k-1} . Hence, the optimal control problem with variable sampling (9) at each time t_k can be rewritten as follows:

$$\begin{aligned} \min_{\substack{u_{0:N-1|k} \\ \beta_k \in \mathbb{R}^2}} & \frac{\hat{J}_k}{w(N, \beta)} \\ \text{s.t.} & x_{k+j+1|k} = x_{k+j|k} + \Delta_{k+j|k} f_c(x_{k+j|k}, u_{k+j|k}), \\ & \Delta_{k+j|k} = w(j+1, \beta_k) - w(j, \beta_k), \\ & \underline{\alpha} T \leq w(N, \beta_k) \leq \bar{\alpha} T, \\ & -\beta_1 < 0, -\beta_2 \leq 0, \\ & SOC_{min} \leq x_{k+j|k} \leq SOC_{max}, \\ & 0 \leq u_{k+j|k} \leq Q_n, \\ & \underline{P}(x_{k+j|k}) \leq u_{k+j|k} - w_f(t_{k+j}) \leq \bar{P}(x_{k+j|k}), \\ & \forall j = 0, \dots, N-1 \text{ with given } x_k, \end{aligned} \quad (16)$$

where the objective $\frac{\hat{J}_k}{w(N, \beta)}$ indicates the average cost over the entire prediction horizon $[0, w(N, \beta)]$.

B. Result

The parameters are: $N = 10$, $T = 1$ hour, $Q_n = 400$ MWh, $\underline{\alpha} = 1$, $\bar{\alpha} = 4$, $SOC_{min} = 0.3$, $SOC_{max} = 0.9$, $x(0) = 0.4$. When $Q_c \leq Q_n$, the battery charge and discharge limits are defined as follows [21]:

$$\bar{P}(x) = Q_c x, \quad \underline{P}(x) = Q_c(x-1), \quad x \in [0, 1]. \quad (17)$$

When $Q_c > Q_n$, the limits are defined by

$$\bar{P}(x) = \begin{cases} Q_c x, & x \in [0, \frac{Q_n}{Q_c}] \\ Q_n, & x \in [\frac{Q_n}{Q_c}, 1] \end{cases}, \quad (18)$$

and

$$\underline{P}(x) = \begin{cases} -Q_n, & x \in [0, 1 - \frac{Q_n}{Q_c}] \\ Q_c(x-1), & x \in [1 - \frac{Q_n}{Q_c}, 1] \end{cases}. \quad (19)$$

The simulation's time step is 0.1 hour and the entire

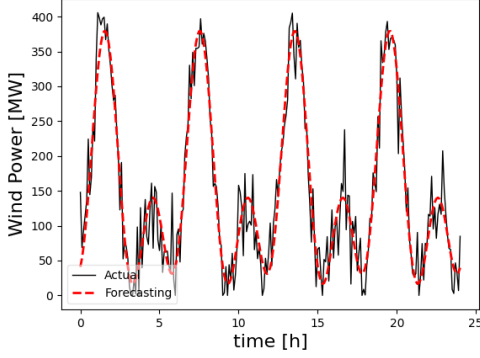


Fig. 3: The actual and forecasting wind power trajectories. $w_f(t) = 120\sin(\frac{\pi t}{3}) + 100\sin(2\pi\frac{t+2}{3} + 0.4) + 150$. The actual wind $w_a(t)$ equals to the forecasting $w_t(t)$ adding a random noise whose distribution is $\mathcal{N}(0, 40^2)$. The actual wind is clipped to zero when negative.

simulation horizon is 24 hours. The wind trajectories are shown in Fig. 3. Ref. [21] also proposes a heuristic control algorithm, which is written as follows:

$$u(t) = w_f(t) \cdot 2x(t). \quad (20)$$

This section adopts both the heuristic control algorithm and an MPC strategy with uniform sampling for revenue comparisons. The prediction horizon for the MPC with uniform sampling is 1 hour and includes 10 steps.

Fig. 4 compares the average revenue (the converse of the total cost) given different battery capacities and control strategies when wind forecasting is perfect. The battery capacity varies from 200 MWh (50% of the nameplate) to 1200 MWh (300%). And all the average revenues are normalized as the revenue of 200 MWh given uniform sampling MPC is set to 1. Fig. 4 shows that the proposed VS-MPC strategy outperforms the other two methods for all battery capacities listed in the figure. As the battery capacity increases, the revenue for two MPC strategies increases because a battery with a larger capacity is more capable of compensating for wind intermittency. The revenue difference between the two MPC strategies is roughly constant as the battery capacity grows. Since the maximum length of the prediction horizon for VS-MPC is fixed over these cases, the exclusive look-ahead information that VS-MPC obtains is nearly the same. And the revenue difference between the heuristic control algorithm and MPC strategies grows when the battery capacity rises because the heuristic algorithm does not exploit any look-ahead information.

Fig. 5 compares the average revenue given different battery sizes and control strategies when wind forecasting is imperfect (wind trajectories shown in Fig. 3). Fig. 5 also reveals that the VS-MPC strategy outperforms the other two methods for all battery capacities. And all the other observations are consistent with those mentioned in Fig. 4.

Fig. 6 shows the trajectories of the control input (power scheduling) and the state (SOC) for 3 methods when Q_c

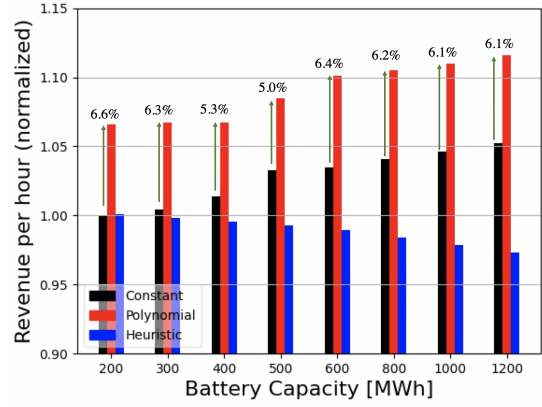


Fig. 4: Average revenue (normalized) when wind forecasting is perfect. The number over the red bar is the relative difference in revenue between the two MPC strategies.

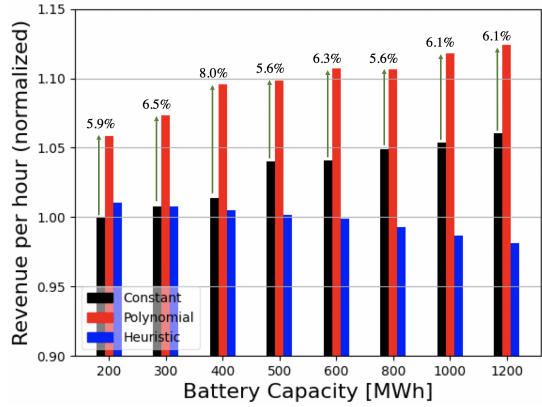
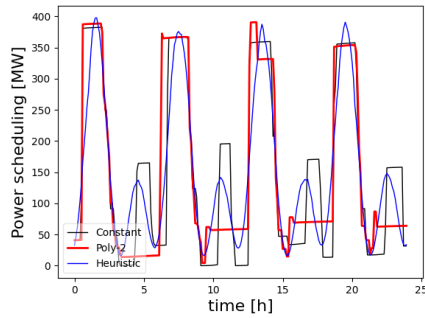


Fig. 5: Average revenue (normalized) when wind forecasting is imperfect

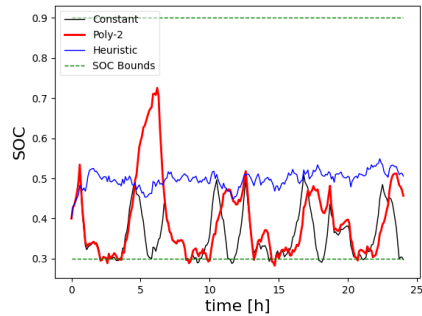
= 400 MWh. Since the heuristic algorithm does not use any prediction, its SOC oscillates around 0.5 due to the forecasting error. Since it does not use much battery capacity for compensating wind intermittency, its average revenue underperforms the MPC strategies. As for the VS-MPC, since it is possible to exploit much more look-ahead information by a longer horizon, its behavior around 5, 10, 17, and 22 hours is more smooth than the uniform sampling MPC, which reduces the ramping cost.

V. CONCLUSION

This paper proposes a variable sampling model predictive control (VS-MPC) strategy, which can deal with multi-timescale systems with only one controller. Unlike the existing non-uniform sampling MPC (NS-MPC) or multi-horizon MPC (MH-MPC) strategies, VS-MPC does not require offline and manual tuning on some parameters for the prediction horizon. Instead, VS-MPC constructs a differentiable and parameterized time-warping function to describe the sampling nature of a non-uniform horizon. Then an optimization program jointly determines the optimal control inputs and the parameters for the time-warping function at each timestamp. Lastly, this paper uses an example of BESS



(a) The trajectories of input for 3 methods.



(b) The trajectories of SOC for 3 methods.

Fig. 6: Details about the BESS system when the wind forecasting is imperfect. $Q_c = 400$ MWh.

for a wind farm to demonstrate the performance of VS-MPC. Some revenue comparisons for several methods have been provided to show the advantages of the proposed VS-MPC. Future work includes an extension of the proposed VS-MPC to be tunable concerning additional loss or constraints [23], [24], cooperative tuning of VS-MPC for multi-agent systems [25], and application of VS-MPC into other practical systems such as battery management systems [26].

REFERENCES

- [1] J. H. Lee, "Model predictive control: Review of the three decades of development," *International Journal of Control, Automation and Systems*, vol. 9, no. 3, pp. 415–424, 2011.
- [2] W. C. Clarke, C. Manzie, and M. J. Brear, "Hierarchical economic mpc for systems with storage states," *Automatica*, vol. 94, pp. 138–150, 2018.
- [3] Z. Wei, J. Zhao, D. Ji, and K. J. Tseng, "A multi-timescale estimator for battery state of charge and capacity dual estimation based on an online identified model," *Applied energy*, vol. 204, pp. 1264–1274, 2017.
- [4] J. P. Koeln, H. C. Pangborn, M. A. Williams, M. L. Kawamura, and A. G. Alleyne, "Hierarchical control of aircraft electro-thermal systems," *IEEE transactions on control systems technology*, vol. 28, no. 4, pp. 1218–1232, 2019.
- [5] W. Wang and J. P. Koeln, "Hierarchical multi-timescale energy management for hybrid-electric aircraft," in *Dynamic Systems and Control Conference*, vol. 84270, p. V001T11A002, American Society of Mechanical Engineers, 2020.
- [6] I. Askari, B. Badnava, T. Woodruff, S. Zeng, and H. Fang, "Sampling-based nonlinear mpc of neural network dynamics with application to autonomous vehicle motion planning," in *2022 American Control Conference (ACC)*, pp. 2084–2090, IEEE, 2022.
- [7] M. R. Amini, I. Kolmanovsky, and J. Sun, "Hierarchical mpc for robust eco-cooling of connected and automated vehicles and its application to electric vehicle battery thermal management," *IEEE Transactions on Control Systems Technology*, vol. 29, no. 1, pp. 316–328, 2020.
- [8] Q. Hu, M. R. Amini, I. Kolmanovsky, J. Sun, A. Wiese, and J. B. Seeds, "Multihorizon model predictive control: An application to integrated power and thermal management of connected hybrid electric vehicles," *IEEE Transactions on Control Systems Technology*, vol. 30, no. 3, pp. 1052–1064, 2021.
- [9] P. Kokotović, H. K. Khalil, and J. O'reilly, *Singular perturbation methods in control: analysis and design*. SIAM, 1999.
- [10] M. Farina, X. Zhang, and R. Scattolini, "A hierarchical multi-rate mpc scheme for interconnected systems," *Automatica*, vol. 90, pp. 38–46, 2018.
- [11] H. C. Pangborn, C. E. Laird, and A. G. Alleyne, "Hierarchical hybrid mpc for management of distributed phase change thermal energy storage," in *2020 American Control Conference (ACC)*, pp. 4147–4153, IEEE, 2020.
- [12] Q. Hu, M. R. Amini, A. Wiese, M. Tascillo, J. B. Seeds, I. Kolmanovsky, and J. Sun, "A spatial data-driven vehicle speed prediction framework for energy management of hevs using multi-horizon mpc with non-uniform sampling," in *2022 American Control Conference (ACC)*, IEEE, 2022.
- [13] C. K. Tan, M. J. Tippet, and J. Bao, "Model predictive control with non-uniformly spaced optimization horizon for multi-timescale processes," *Computers & Chemical Engineering*, vol. 84, pp. 162–170, 2016.
- [14] O. Gomozov, J. P. F. Trovao, X. Kestelyn, and M. R. Dubois, "Adaptive energy management system based on a real-time model predictive control with nonuniform sampling time for multiple energy storage electric vehicle," *IEEE Transactions on Vehicular Technology*, vol. 66, no. 7, pp. 5520–5530, 2016.
- [15] D. Liao-McPherson, S. Kim, K. Butts, and I. Kolmanovsky, "A cascaded economic model predictive control strategy for a diesel engine using a non-uniform prediction horizon discretization," in *2017 IEEE Conference on Control Technology and Applications (CCTA)*, pp. 979–986, IEEE, 2017.
- [16] T. Brüdigam, D. Prader, D. Wollherr, and M. Leibold, "Model predictive control with models of different granularity and a non-uniformly spaced prediction horizon," in *2021 American Control Conference (ACC)*, pp. 3876–3881, IEEE, 2021.
- [17] H. Sakoe and S. Chiba, "Dynamic programming algorithm optimization for spoken word recognition," *IEEE transactions on acoustics, speech, and signal processing*, vol. 26, no. 1, pp. 43–49, 1978.
- [18] P. Kingston and M. Egerstedt, "Time and output warping of control systems: Comparing and imitating motions," *Automatica*, vol. 47, no. 8, pp. 1580–1588, 2011.
- [19] W. Jin, T. D. Murphey, D. Kulić, N. Ezer, and S. Mou, "Learning from sparse demonstrations," *IEEE Transactions on Robotics*, 2022.
- [20] M. I. Rosen, "Niels hendrik abel and equations of the fifth degree," *The American Mathematical Monthly*, vol. 102, no. 6, pp. 495–505, 1995.
- [21] C.-T. Li, H. Peng, and J. Sun, "Mpc for reducing energy storage requirement of wind power systems," in *2013 American Control Conference*, pp. 6607–6612, IEEE, 2013.
- [22] I. M. Monitor, "2010 state of the market report for the miso electricity markets," 2011.
- [23] W. Jin, Z. Wang, Z. Yang, and S. Mou, "Pontryagin differentiable programming: An end-to-end learning and control framework," in *Advances in Neural Information Processing Systems*, vol. 33, pp. 7979–7992, 2020.
- [24] W. Jin, S. Mou, and G. J. Pappas, "Safe pontryagin differentiable programming," in *Advances in Neural Information Processing Systems*, vol. 34, pp. 16034–16050, 2021.
- [25] Z. Lu, W. Jin, S. Mou, and B. D. O. Anderson, "Cooperative tuning of multi-agent optimal control systems," in *2022 IEEE 61st Conference on Decision and Control (CDC)*, pp. 571–576, 2022.
- [26] N. Tian, H. Fang, and Y. Wang, "Real-time optimal lithium-ion battery charging based on explicit model predictive control," *IEEE Transactions on Industrial Informatics*, vol. 17, no. 2, pp. 1318–1330, 2021.